Tu P7 07

Adaptive Finite Difference for Seismic Wavefield Modelling

G. Yao* (Imperial College London), H.A. Debens (Imperial College London), A. Umpleby (Imperial College London) & M. Warner (Imperial College London)

SUMMARY

We present an alternative scheme for calculating finite difference coefficients in seismic wavefield modelling. This novel technique seeks to minimise the difference between the accurate value of spatial derivatives and the value calculated by the finite difference operator over all propagation angles. Since the coefficients vary adaptively with different velocities and source wavelet bandwidths, the method maximises the accuracy of the finite difference operator. Numerical examples demonstrate that this method is superior to standard finite difference methods whilst comparable to Zhang's optimised finite difference method.

Introduction

Seismic wavefield modelling is an essential component of advanced seismic imaging (Yao and Jackubowciz 2012), model building, and full waveform inversion (Warner et al. 2013). The most popular modelling method is finite difference, because it is simple to implement and highly efficient compared to other techniques, such as finite element. However, finite-difference methods suffer from numerical dispersion, which causes wavefronts of different frequencies to travel at different speeds (Liu and Sen 2009). For standard finite-difference implementations, the higher the frequency the stronger the dispersion. To mitigate this dispersion, optimisation strategies are often employed to find better finite-difference coefficients that cover a wider frequency and wavenumber range with limited errors. These enhanced methods try either to fit the accurate operator (Zhang and Yao 2012; Chu and Stoffa 2012; Stork 2013) or to minimise the dispersion of the time and space terms (Etgen 2007; Liu 2013; Wang et al. 2014).

In this paper, we present a means to calculate optimal finite-difference coefficients that can be applied in a wide range of circumstances.

Theory

The simplest 2D wave equation can be expressed as

$$\frac{1}{v^2}\frac{\partial^2 u}{\partial t^2} = \frac{\partial^2 u}{\partial x^2} + \frac{\partial^2 u}{\partial z^2} + s(t). \quad (1)$$

Solving Equation 1 with finite-difference methods entails the use of finite-difference operators to calculate numerically the temporal and spatial second derivatives. Time-recursive schemes are usually used to calculate wavefields explicitly from one time step to the next. In order to save compute memory, 2nd-order finite difference is commonly applied to the temporal derivative. As a result, improvement to accuracy and reduction of numerical dispersion relies on the selection of the finite-difference operator for the spatial derivatives. A sensible choice is high-order finite difference, which can be written as

$$\frac{\partial^2 u}{\partial x^2} + \frac{\partial^2 u}{\partial z^2} \approx \sum_{i=-N}^{N} \left[\frac{1}{\Delta x^2} c_x(i)\, u(x + i\Delta x, z, t) + \frac{1}{\Delta z^2} c_z(i)\, u(x, z + i\Delta z, t)\right], \quad (2)$$

where c_x and c_z are finite-difference coefficients for the x and z derivatives, $2N$ is the accuracy order of the finite-difference operator, and Δx and Δz are sampling intervals. The desired values of c_x and c_z make the right-hand side of Equation 2 approximately equal to the left-hand side terms for waves propagating in any direction. Since the finite-difference stencils for the x and z directions have the same form, it is sensible to assume that c_x equals c_z. As a result, we only need to find c_x for a wave travelling in any direction by solving

$$\frac{\partial^2 u}{\partial x^2} \approx \sum_{i=-N}^{N} \frac{1}{\Delta x^2} c_x(i)\, u(x + i\Delta x, z, t). \quad (3)$$

Since seismic wavefields are band-limited, c_x only needs to cover this bandwidth, which can be determined by the known source wavelet, $s(t)$. For a given velocity and propagation direction, the waveform of a plane wave formed by $s(t)$ can be analytically or numerically calculated, assuming the form $s(x, \theta)$. As a result, the second derivative, $b(x, \theta)$, of the wave along the x-axis can also be analytically or numerically calculated. The pseudo-spectrum method (Kosloff and Baysal 1982) gives a precise numerical solution of $b(x, \theta)$ up to the Nyquist frequency. Thus the only unknown in Equation 3 is c_x, which can therefore be found by minimising the objective function

$$\phi = \int_{\theta=0}^{\pi/2} \int_{x=0}^{l} \left\| b(x, \theta) - \sum_{i=-N}^{N} \frac{1}{\Delta x^2} s(x + i\Delta x, \theta) c_x(i) \right\|^2 dx d\theta. \quad (4)$$

where θ is the wave propagation angle and l is the waveform duration. A fixed-bandwidth wavelet produces different wavelengths for different velocities; therefore the finite-difference coefficients also change with velocity. For a heterogeneous velocity model, a table of finite-difference coefficients for different velocity values can be created before modelling. During the modelling, the appropriate coefficient can be looked-up quickly from the table because the table itself is small and can be

efficiently held in cache. Wavelets with identical amplitude spectra give the same finite-difference coefficients by Equation 4. If the weights for all frequencies are expected to be identical, then the low-pass filtered version of a spike, with the same bandwidth as $s(t)$, can be used as the wavelet in Equation 4. Since our finite-difference coefficients adaptively change with wavelet bandwidth and velocity, this finite difference method is referred to here as adaptive finite difference.

Examples

The first example demonstrates adaptive finite difference using a homogenous velocity model of 2000 m/s. A 13-Hz Ricker wavelet with 0.5 ms sampling interval is chosen as the source wavelet which is located at the centre of the model. The cell size is 20 m for both x and z directions. A low-pass filtered version of a spike with bandwidth from 0 to 32 Hz is chosen as the wavelet for Equation 4 to calculate the finite-difference coefficients. Every 4 degrees from 2 to 90 degrees is used when minimising Equation 4. The errors (Chu and Stoffa 2012) of the 12^{th}-order adaptive operator, the $8^{th}/12^{th}/24^{th}$ /36^{th}-order standard operators, and 12^{th}-order Zhang's optimised operator are illustrated in Figure 1. Figure 1b demonstrates that, in the region of error less than $\pm 1.5e^{-4}$, the adaptive finite difference and Zhang's optimised finite difference both cover a broader wavenumber range than the $8^{th}/12^{th}/24^{th}$-order standard finite difference and give a good approximation to close to 36^{th}-order.

The adaptive finite difference has smaller errors for low wavenumbers than Zhang's optimised finite difference, but slightly larger errors for higher wavenumbers. As a result, the adaptive finite difference is more accurate for low-wavenumber waves. This is particularly useful for events propagating with a large angle to the x- or z-axes. Standard finite different has a good accuracy for low wavenumbers but huge errors for high wavenumbers. To achieve broader coverage, optimised finite-difference operators distribute the errors to a broader wavenumber range in a least-squares sense. This is the reason why optimised finite-difference methods often out-perform standard finite difference methods.

Figure 2 shows wavefield snapshots at 4.5 and 9.5 seconds. As can be seen in Figures 2 and 3, standard finite difference has stronger dispersion than the adaptive and Zhang's optimised finite difference. The pseudo-spectral method achieves the smallest dispersion, because it calculates spatial derivatives precisely up to the Nyquist wavenumber. If the pseudo-spectral result is used as a reference, then adaptive finite difference gives the smallest total RMS error, which indicates the difference to the reference wavefield. However, Zhang's optimised finite difference achieves the smallest RMS error in the directions close to x- and z-axes, because in this particular example the wavenumber content is high in these directions.

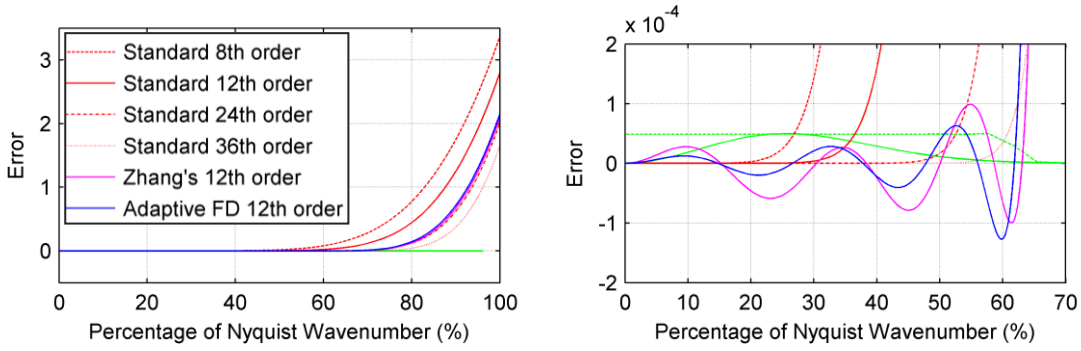

(a) (b)

Figure 1 *(a) Comparison of the errors for standard, Zhang's and adaptive finite difference operators for a 13Hz Ricker wavelet in a 2000 m/s constant velocity model with a 20 m cell size. (b) Zoomed window of (a). The red, blue and magenta curves represent the standard operators, and the 12^{th}-order adaptive and Zhang's finite difference operators, respectively. The solid green curve represents the spectrum of the Ricker wavelet mapped into wavenumber. The dashed green curve represents the spectrum of the band-limited wavelet used for the adaptive finite difference operator calculation.*

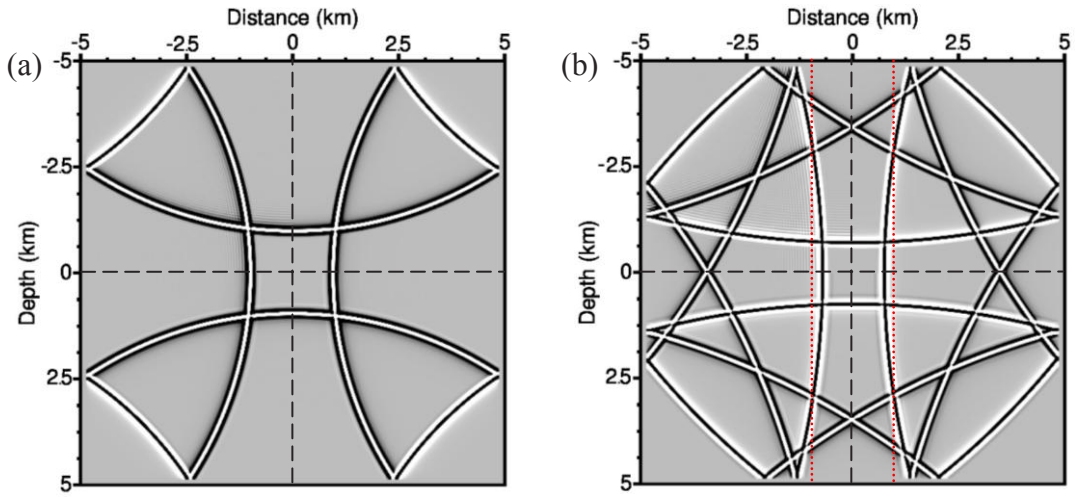

Figure 2 *Snapshots of wavefields at (a) 4.5 seconds and (b) 9.5 seconds. The model has a constant velocity of 2000 m/s; the wavelet is a 13Hz Ricker wavelet; temporal and spatial sampling intervals are 0.5 ms and 20 m, respectively. The top-left quadrant is generated by 12th-order standard finite-difference method. The bottom-left quadrant is given by 12th-order Zhang's finite-difference method. The bottom-right quadrant is produced by the 12th-order adaptive finite-difference method. The top-right quadrant is generated by the pseudo-spectral method. The displays are clipped to 5% of the maximum amplitude. Standard finite difference can be seen to produce more pronounced dispersion than the other three methods.*

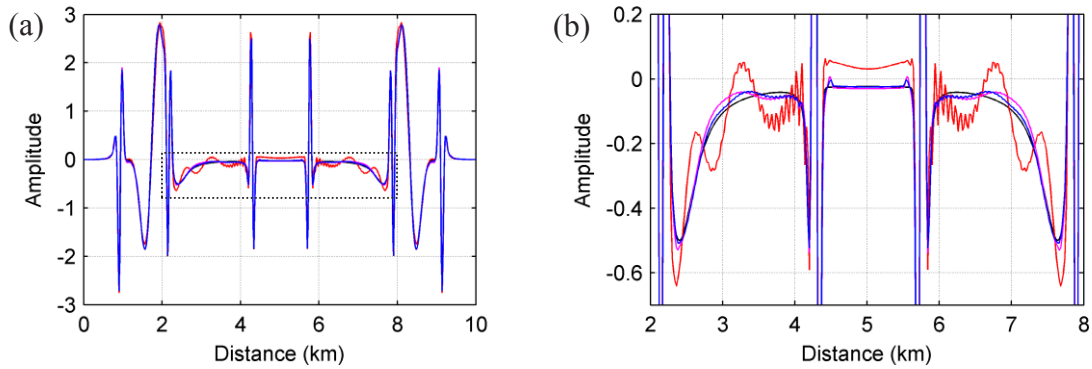

Figure 3 *(a) Comparison of the waveform represented by the two vertical dotted red lines in Figure 2b. (b) Zoomed window of (a) indicated by box. The black curve represents the result of the pseudo-spectral method. The other colours match those in Figure 1. As can be seen, adaptive finite-difference and Zhang's optimised finite-difference methods produce waveforms closer to the pseudo-spectral method than the standard finite-difference method.*

The second example is to apply the four methods to the Marmousi model with a 15 m spacing interval. A 13Hz Ricker wavelet with 0.5 ms sampling interval is used as the source wavelet. In order to control the oscillations of the finite-difference error to around $\pm 1e^{-4}$, which is a sensible objective as made by Zhang and Yao (2012), a low-pass filtered version of a spike with bandwidth from 0 to 32 Hz is used to calculate the adaptive finite-difference coefficients for velocities varying from 1500 m/s to 4700 m/s with a 100 m/s increment. Figure 4b shows the records for a trace at a distance of 9 km and a depth of 200 m for all four methods. If the result of the pseudo-spectral method is used as a reference, the differences are shown in Figure 4c. It is clear to see that the standard finite-difference result has big errors around 6.2 to 6.8 seconds. In fact, the data in this region are dominated by direct arrivals, which travel through water with a velocity of 1500 m/s. Because the velocity is low, the wavenumber is large, and standard finite different has substantial errors for large wavenumbers (Figure 1b). Consequently, the standard finite difference result has big errors. In contrast, both adaptive and Zhang's optimised finite difference results have much smaller errors for the direct arrival. In high velocity areas, however, the adaptive finite difference result is even more accurate because the wavenumber of the wavefield becomes smaller and adaptive finite difference changes the coefficients

to cover a smaller wavenumber range than Zhang's optimised finite difference in these areas, so that the adaptive finite difference has smaller oscillation errors. This is demonstrated in the early and late arrivals, which travel deeper and in higher velocity areas.

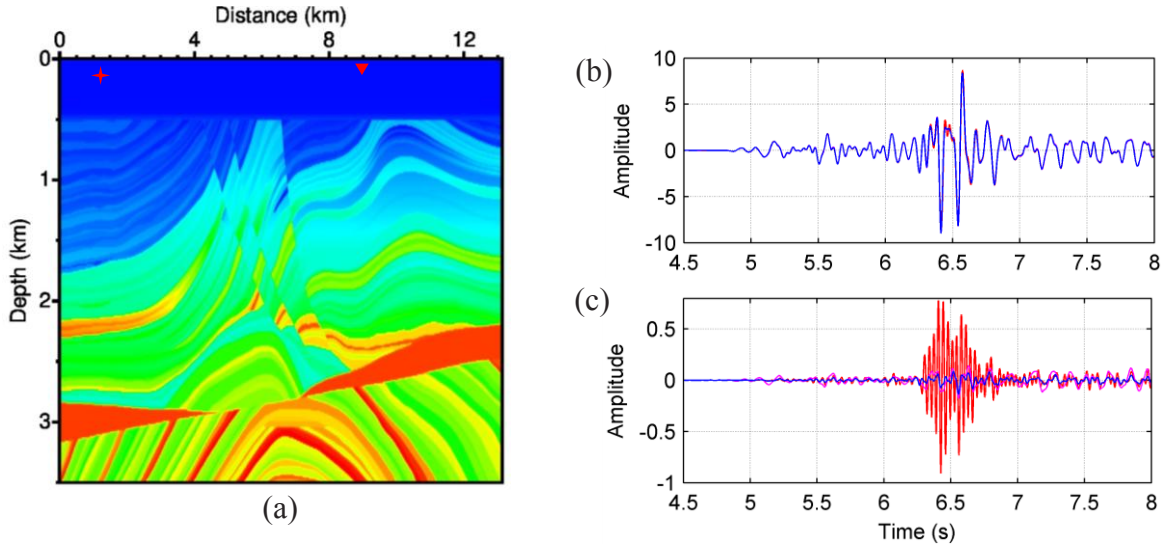

Figure 4 *12th-order adaptive, Zhang's and standard finite difference methods and pseudo-spectral method applied to (a) the Marmousi model. The source is located at a distance of 1.2 km and a depth of 200 m (indicated by the red star); the receiver is positioned at a distance of 9 km and a depth of 200 m (indicated by the red triangle). (b) The records of the four methods and (c) the differences between the finite-difference and pseudo-spectral records. The colours match those in Figure 3. It is clear to see that the standard method has larger errors, and the adaptive method has smaller errors.*

Discussion and Conclusion

We have presented an improved way to calculate finite-difference coefficients. Since this new method generates the coefficients adaptively relative to the bandwidth of the source wavelet and media velocity, it can maximise the accuracy for a given length operator. The two examples presented demonstrate it is a large improvement over standard finite-difference methods, and superiority over Zhang's optimised finite-difference method in some circumstances. This method of calculating finite-difference coefficients can be used with any order of derivative, including fractional orders and irregularly spaced stencils. It is possible to extend this technique to consider time-space dispersion.

References

Chu, C. and Stoffa, P. [2012] Determination of finite-difference weights using scaled binomial windows. *Geophysics*, 77(3), W17-W26.

Etgen, J. T. [2007] A tutorial on optimizing time domain finite-difference schemes: "Beyond Holberg". *Stanford Exploration Project*, Report 129, 33–43.

Kosloff, D. and Baysal, E. [1982] Forward modeling by a Fourier method. *Geophysics*, 47(10), 1402-1412.

Liu, Y. [2013] Globally optimal finite-difference schemes based on least squares. *Geophysics*, 78(4), T113-T132.

Liu, Y. and Sen, M. K. [2009] Advanced finite-difference methods for seismic modeling. *Geohorizons*, 14(2).

Stork, C. [2013] Eliminating nearly all dispersion error from FD modeling and RTM with minimal cost increase. *75th EAGE Conference & Exhibition*, Extended Abstracts, Tu1107

Wang, Y., Liang, W., Nashed, Z.,...,Yang, C. [2014] Seismic modeling by optimizing regularized staggered-grid finite-difference operators using a time-space-domain dispersion-relationship-preserving method. *Geophysics*, 79(5), T277-T285.

Warner, M., Ratcliffe, A., Nangoo, T.,...,Betrand, A. [2013] Anisotropic 3D full-waveform inversion. *Geophysics*, 78(2), R59-R80.

Yao, G. and Jackubowciz, H. [2012] Least-Squares Reverse-Time Migration. *74th EAGE Conference & Exhibition*, Expanded Abstracts, X043.

Zhang, J. and Yao, Z. [2012] Optimized finite-difference operator for broadband seismic wave modeling. *Geophysics*, 78(1), A13-A18.